STANDARD ARTICLE

Journal of Veterinary Internal Medicine ACVIM

American College of Veterinary Internal Medicine

Relationship of microsatellite instability to mismatch repair deficiency in malignant tumors of dogs

Sakuya Inanaga[1] | Masaya Igase[1] | Yusuke Sakai[2] | Kenji Hagimori[3] |
Hiroshi Sunahara[4] | Hiro Horikirizono[5] | Kazuhito Itamoto[6] | Kenji Baba[7] |
Yoshiharu Ohsato[8] | Takuya Mizuno[1]

[1]Laboratory of Molecular Diagnostics and Therapeutics, Joint Faculty of Veterinary Medicine, Yamaguchi University, Yamaguchi, Japan

[2]Department of Pathology, National Institute of Infectious Diseases, Tokyo, Japan

[3]Kyoto Animal Medical Center, Kyoto, Japan

[4]Laboratory of Veterinary Surgery, Joint Faculty of Veterinary Medicine, Yamaguchi University, Yamaguchi, Japan

[5]Laboratory of Veterinary Radiology, Joint Faculty of Veterinary Medicine, Yamaguchi University, Yamaguchi, Japan

[6]Laboratory of Companion Animal Medicine, Joint Faculty of Veterinary Medicine, Yamaguchi University, Yamaguchi, Japan

[7]Laboratory of Veterinary Internal Medicine, Joint Faculty of Veterinary Medicine, Yamaguchi University, Yamaguchi, Japan

[8]Kahotechno Co., Ltd., Fukuoka, Japan

Correspondence
Takuya Mizuno, Laboratory of Molecular Diagnostics and Therapeutics, The United Graduate School of Veterinary Medicine, Yamaguchi University, 1677-1 Yoshida, Yamaguchi, Yamaguchi 753-8511, Japan.
Email: mizutaku@yamaguchi-u.ac.jp

Funding information
Japan Society for the Promotion of Science, Grant/Award Number: KAKENHI Grant Number 21H04754.

Abstract

Background: Microsatellite instability (MSI) is a type of genomic instability caused by mismatch repair deficiency (dMMR) in tumors. Studies on dMMR/MSI are limited, and the relationship between dMMR and MSI is unknown in tumors of dogs.

Objectives: We aimed to identify the frequency of dMMR/MSI by tumor type and evaluate the relationship between dMMR and MSI in tumors of dogs.

Animals: In total, 101 dogs with 11 types of malignant tumors were included.

Methods: We extracted DNA from fresh normal and tumor tissues. Twelve microsatellite loci from both normal and tumor DNA were amplified by PCR and detected by capillary electrophoresis. Each microsatellite (MS) was defined as MSI if a difference in product size between the tumor and normal DNA was detected. The dMMR was evaluated by immunohistochemistry with formalin-fixed paraffin-embedded tumor tissues. Next, we confirmed whether dMMR induces MSI by serial passaging of MMR gene knockout cell lines for 3 months.

Results: Microsatellite instability was detected frequently in oral malignant melanoma. The number of MSI-positive markers was higher in cases with dMMR than in

those with proficient MMR ($P < .0001$). Statistical analysis indicated that the occurrence of MSI in FH2305 might have relevance to dMMR. Furthermore, MSI occurred in dMMR cell lines 3 months after passaging.

Conclusions and Clinical Importance: Microsatellite instability and dMMR more frequently were found in oral malignant melanoma than in other tumors, and dMMR has relevance to MSI in both clinical cases and cell lines.

KEYWORDS

dogs, genomic instability, loss of heterozygosity, oral malignant melanoma

1 | INTRODUCTION

Microsatellites (MS) are short repetitive sequences composed of 1 to 6 base pairs dispersed throughout noncoding regions in the genome.[1] Microsatellite instability (MSI) is a condition in which replication errors, such as insertions and deletions, accumulate in MS and cause differences in MS repeats between normal and tumor tissues. In humans, MSI is detected in some patients with various tumors, particularly Lynch syndrome,[2] which is a hereditary disease caused by a congenital dysfunction of DNA mismatch repair (MMR) system, referred to as mismatch repair deficiency (dMMR). Patients with this disease tend to develop tumors. Hence, it was suspected that MSI is related to carcinogenesis, regardless of tumor type. In a previous study, MSI was detected in 4/35 (11%) of dogs with mammary gland tumors,[3] but the MMR system was not analyzed in that study. Previously, it was determined that dMMR tended to occur in oral malignant melanoma and hepatocellular carcinoma in dogs.[4] To the best of our knowledge, no reports have comprehensively analyzed MSI in various tumors of dogs and evaluated its relationship with dMMR.

Microsatellite instability mostly is induced by dMMR. The MMR system preserves genomic stability and is mainly regulated by 4 genes: *msh2*, *msh6*, *mlh1*, and *pms2*.[5] Mismatch repair deficiency is caused by a germline mutation (ie, Lynch syndrome), somatic mutation, or hypermethylation of these MMR genes in various tumors.[6-10] It is known that dMMR increases tumor mutation burden and MSI, leading to carcinogenesis.[11-14] In humans, dMMR and MSI are simultaneously examined by immunohistochemistry (IHC) and PCR to understand genetic mechanisms in carcinogenesis.[15] In addition, numerous reports showed that tumors with dMMR and MSI are highly responsive to immune checkpoint inhibitors (ICIs).[16-18] Therefore, dMMR/MSI serves as a predictive biomarker of the likely efficacy of ICIs.[19] Furthermore, PCR for MS also provides information about loss of heterozygosity (LOH). Loss of heterozygosity is another type of genomic instability and is caused by various mechanism such as somatic mutations, errors of meiosis, and mitotic recombination. It is known to be associated with tumors and developmental disorders.[20-22] Thus, LOH is considered a prognostic biomarker in patients with tumors, independent of MSI.[23]

We evaluated MSI status in several types of tumors to identify tumor types that frequently have MSI, including its relationship with

dMMR in clinical cases and cell lines. Based on these data, MS loci suitable for MSI analysis were narrowed down to make the analysis more productive and accurate. Furthermore, LOH was analyzed simultaneously with MSI because only few reports have examined LOH at MS loci in tumors of dogs.

2 | MATERIALS AND METHODS

2.1 | Clinical samples

Clinical samples were obtained from tumor-bearing dogs that came to Yamaguchi University Animal Medical Center and Kyoto Animal Medical Center for diagnosis or treatment from May 2020 to March 2021. All dogs underwent biopsy or surgical resection and were diagnosed with malignant tumors by veterinary pathologists at Yamaguchi University or IDEXX Laboratories (Tokyo, Japan), except for some cases with lymphoma that were diagnosed only by cytology. Blood and fresh tumor tissues were collected from each dog to evaluate MSI, and an oral mucosal swab was taken instead of blood to extract normal tissue DNA when tumor cells were observed on a blood smear. Formalin-fixed paraffin-embedded (FFPE) tumor tissues were collected from each dog to evaluate dMMR. The study was approved by the Ethics Committee of Yamaguchi University.

2.2 | PCR for microsatellite sequences

Genomic DNA was extracted from blood (or oral mucosal swab) and fresh tumor tissues with a QIAamp DNA Blood Mini Kit (QIAGEN Tokyo, Tokyo, Japan) or QIAamp DNA Mini Kit (QIAGEN Tokyo), respectively, and was stored at 4°C until further use.

For MSI analysis, 12 MS loci were selected (Table 1)[24,25] because of their high instability rates in a previous report[3] and our preliminary experiments. Microsatellite sequences were amplified from tumor and normal DNA by PCR in 15 μL of reaction volume, including 12 ng of DNA and 2.5 μM of each primer labeled with fluorescent dye using BIOTAQ DNA Polymerase (Meridian Life Science, Inc, Memphis, Tennessee). The PCR amplicons were detected by capillary electrophoresis (3500xL Genetic Analyzer, Thermo Fisher Scientific K.K., Tokyo,

TABLE 1 Primers used for amplification of microsatellite markers in this study

Microsatellite marker	Repeat type	Chromosome	Forward primer	Reverse primer	Fluorescent label
C13.900	Di	CFA 13	TTGGACTTCTAATTTTTCATT	CAACTGACTAAATCTCCTAATG	FAM
PEZ11	Tetra	CFA 8	ATTCTCTGCCTCTCCCTTTG	TGTGGATAATCTCTTCTGTC	FAM
FH2054	Tetra	CFA 12	GCCTTATTCATTGCAGTTAGGG	ATGCTGAGTTTTGAACTTTCCC	PET
C22.763	Di	CFA 22	CAGCCCACTTCCTGGAAATA	GACCAGTGTGCATTAAGCC	HEX
FH2305	Tetra	CFA 30	TCATTGTCTCCCTTTCCCAG	AAGCAGGACATTCATAGCAGTG	FAM
PEZ8	Tetra	CFA 17	TATCGACTTTATCACTGTGG	ATGGAGCCTCATGTCTCATC	PET
FH2175	Tetra	CFA 16	TTCATTGATTTCTCCATTGGC	AGGACTCTAAAAACTTGCCTCC	HEX
FH3837	Tetra	CFA 5	GGCCTCGTAGAATACATTTGG	AGCAAGGAAGGCATCTGG	FAM
FH2594	Tetra	CFA 5	TTTAAGGAGCTGCTCATGCA	CTGAAATTCCTGGCCCAGTA	FAM
FH3113	Tetra	CFA 5	CTGAATTATGGGAAAACATGG	CAGGGAAGGAAGAAAACAGC	HEX
CPH14	Di	CFA 5	GAAAGACAATCCCTGAAATGC	ACCCCATTTATGAGAATCATGT	FAM
AHT137	Di	CFA 11	TACAGAGCTCTTAACTGGGTCC	CCTTGCAAAGTGTCATTGCT	PET

Japan) and analyzed by a software application (Peak Scanner, Thermo Fisher Scientific K.K.). In each MS sequence, electropherograms of tumor and normal DNA were compared and defined as MSI-positive if a difference in product size was detected. In addition, LOH was defined as a ≥35% reduction in the peak of 1 allele in tumor DNA compared to that in normal DNA.[26] The electropherograms of each sample were evaluated independently by 3 observers.

2.3 | Immunohistochemistry for dMMR analysis

As described in a previous report,[4] each FFPE tissue was incubated with mouse monoclonal anti-human MLH1 antibody (clone G168-15, GeneTex, Inc, Irvine, California, diluted at 1:50), rabbit monoclonal anti-human MSH2 antibody (clone SP46, Abcam, Cambridge, UK, diluted at 1:5100), or mouse monoclonal anti-human MSH6 antibody (clone 44/MSH6, BD Transduction Laboratories, San Diego, California, diluted at 1:250). The isotype antibodies, rabbit IgG antibody (clone DA1E, Cell Signaling Technology, Inc, Danvers, Massachusetts) and mouse IgG1 antibody (clone P3.6.2.8.1, eBioscience, Inc, San Diego, California), were used as negative immunostaining controls. A peroxidase stain DAB Kit (Nacalai Tesque, Inc, Kyoto, Japan) was used to visualize the immunoreaction. The sections were counterstained with Mayer's hematoxylin. To bleach the melanocytic granules of melanoma tissues, the sections were incubated in 10% hydrogen peroxide before antigen retrieval. A Simple Stain AEC Solution (Nichirei Bioscience, Inc, Tokyo, Japan) was used to visualize the immunoreaction instead of DAB.

Immunoreactivity was evaluated if the nuclei of the tumor cells were immunostained with each antibody as compared with those in isotype controls. The immunostaining of the normal tissue areas of each sample was used as a control and simultaneously evaluated to confirm positive immunostaining. Negative immunostaining was confirmed when the nuclei of tumor cells showed negative immunostaining. The immunoreactivity of each sample was independently

evaluated by 4 observers. Based on the results of IHC, the MMR status of each case was determined; MMR proficiency (pMMR) was confirmed if all 3 MMR proteins showed positive immunostaining, or dMMR was confirmed if ≥1 proteins showed negative immunostaining based on criteria used in studies of human tissues.[15]

2.4 | Cell culture

Human embryonic kidney (HEK) 293 T-cell line and SV40-immortalized canine gallbladder epithelial cells (kindly provided by Dr. Kenji Baba) were cultured in a Dulbecco's modified Eagle medium (DMEM)-based complete medium (DMEM mixed with 10% fetal bovine serum and 100 units/mL penicillin-streptomycin and 55 μM 2-mercaptoethanol). All cell lines were maintained at 37°C in a humidified CO_2 gas incubator.

2.5 | Establishment of dMMR/MSI cell lines

According to previous reports,[27] CRISPR-Cas9 small guide RNAs (sgRNAs), which target 1 or more of the MMR genes (*mlh1*, *msh2*, and *msh6*), were designed by an online CRISPR design tool (http://zlab.bio/guide-design-resources). The sequences of sgRNAs of canine MLH1, canine MSH2, and canine MSH6 were 5′-GTGGTGAACCG CATCGCGGC, GCGCTTCTTCCAGGCCATGC-3′, and 5′-GAAGTAA GGCCTAAGGTCCA-3′, respectively. These oligonucleotides were synthesized and inserted into a lentiCRISPR v2 plasmid, which was donated by Dr. Feng Zhang (Addgene, Cambridge, Massachusetts, #52961; http://n2t.net/addgene:52961; RRID: Addgene 52961). To produce lentivirus-expressing sgRNAs that target each gene, HEK293T cells were seeded at 3.0×10^5 cells/well on a 6-well plate a day before transfection. On the day of transfection, 1.25 μg of each plasmid was mixed with PEI Max (Polysciences, Inc, Warrington, Pennsylvania) in an OPTI-MEM buffer (Thermo Fisher Scientific K.K.),

incubated for 15 minutes at room temperature, and added onto HEK293T cells. After 24 hours, the supernatant of HEK293T cells was replaced with a DMEM-based complete medium without antibiotics. After another 24 hours, the supernatant containing lentiviruses was collected and transferred onto gallbladder epithelial cells. After 12 hours of infection, the supernatant was replaced with a DMEM-based complete medium, followed by the addition of 0.2 mg/mL hygromycin onto the gallbladder epithelial cells to select stably transduced cells. Individual single clones were isolated by limited dilution method and further analyzed by Western blotting to confirm the knockout of each protein. Based on the results of Western blotting, clones with complete knockout of each MMR gene were selected and passaged >30 times over 3 months after single clone isolation.

2.6 | Western blotting analysis

Each cell line was collected and lysed with an NP-40 lysis buffer (1% NP40, 10 mM Tris HCl [pH 7.5], 150 mM NaCl, 1 mM EDTA). Equal amounts of protein samples (30 μg) were electrophoresed in 7% acrylamide gel before transferring them onto membranes. The membranes were incubated with each primary antibody (same as the antibodies used in IHC) diluted at 1:1000 in 0.5% skimmed milk in Tris Buffered Saline with Tween20 overnight at 4°C. Horseradish peroxidase (HRP)-conjugated anti-mouse IgG antibody (Merck Millipore, Darmstadt, Germany) or HRP-conjugated anti-rabbit IgG antibody (Jackson ImmunoResearch, West Grove, Pennsylvania) was used as a secondary antibody. The membranes were soaked in Western Lightning Plus-ECL (PerkinElmer, Tokyo, Japan) to visualize the immunoreaction. Immunoreactive bands were quantified and analyzed using AMERSHAM Image Quant 800 (Global Life Sciences Technologies Japan, Tokyo, Japan). The membranes were reused with mouse monoclonal anti-beta actin antibody (Sigma-Aldrich Japan K.K., Tokyo, Japan) to verify equal loading of proteins in each lane.

2.7 | Statistical analysis

Statistical analysis was performed by JMP Pro 15 software (JMP Japan, Tokyo, Japan). A Wilcoxon rank-sum test was conducted to determine the association between the number of MSI-positive markers and dMMR/pMMR status. Statistical significance was set at $P < .05$.

A least absolute shrinkage and selection operator (LASSO) regression model and decision tree model were fitted to further select important variables for the association between dMMR/pMMR status (dependent variable) and MSI-positive markers (independent variables). The LASSO regression model shrank all regression coefficients toward zero and set the coefficients of irrelevant variables to zero according to the regulation weight λ. The optimal value of λ was determined by a 5-fold cross validation. The decision tree analysis used the same variables as LASSO (dMMR/pMMR status as dependent variable and MSI-positive markers as independent variable). The

TABLE 2 Classification of tumor tissues included in this study

Tumor type	Number of cases
Oral malignant melanoma	25
Melanotic	18
Amelanotic	7
Lymphoma	13
T-cell	3
B-cell	8
non-T non-B	2
Mast cell tumor	3
Low grade	3
Mammary gland carcinoma	4
Simple carcinoma	4
Urothelial carcinoma	5
Urinary bladder to urethra	5
Hepatocellular carcinoma	9
Poorly differentiated	1
Moderately differentiated	1
Well-differentiated	7
Squamous cell carcinoma	9
Adenocarcinoma	7
Apocrine gland anal sac adenocarcinoma	2
Lung adenocarcinoma	3
Ceruminous adenocarcinoma	1
Thyroid adenocarcinoma	1
Hemangiosarcoma	3
Soft tissue sarcoma	11
Fibrosarcoma	4
Perivascular wall tumor	3
Leiomyosarcoma	1
Liposarcoma	1
Myxosarcoma	1
Undifferentiated pleomorphic sarcoma	1
Others	12
Osteosarcoma	1
Gastrointestinal stromal tumor	1
Spleen interstitial tumor	1
Histiocytic sarcoma	1
Carcinosarcoma	1
Undifferentiated malignant tumor	2
Intranasal carcinoma	1
Carcinoma nos	3
Sarcoma nos	2
Total	101

tuning parameters were determined by a 5-fold cross validation. Ten cases with other tumors (Table 2) were excluded in the LASSO regression and the decision tree model analyses.

3 | RESULTS

3.1 | Study population

In our study, 101 dogs with tumors were included. The characteristics of these dogs are shown in Table S1, Supporting Information. The population consisted of 51 males (27 castrated) and 50 females (38 spayed). Median age at diagnosis was 11 years and 11 months (range, 5-16 years and 10 months). The cases were classified into 25 cases of oral malignant melanoma, 13 cases of lymphoma, 3 cases of mast cell tumor, 4 cases of mammary gland carcinoma, 5 cases of urothelial carcinoma, 9 cases of hepatocellular carcinoma, 9 cases of squamous cell carcinoma, 7 cases of adenocarcinoma, 3 cases of hemangiosarcoma, 11 cases of soft tissue sarcoma, and 12 cases of other tumors (Table 2). Four lymphoma cases (cases 27, 29, 37, and 38 in Table S1) and 1 urothelial carcinoma case (case 46 in Table S1) had been treated before the tissues were collected for the study.

3.2 | Microsatellite analysis for clinical cases

The results of MSI and LOH are shown in Table S1. Microsatellite instability was defined as an alteration in the peak size of MS amplicons in tumor DNA compared to that in normal DNA (Figure 1). At least 1 MSI-positive marker was detected in 20 cases of oral malignant melanoma,
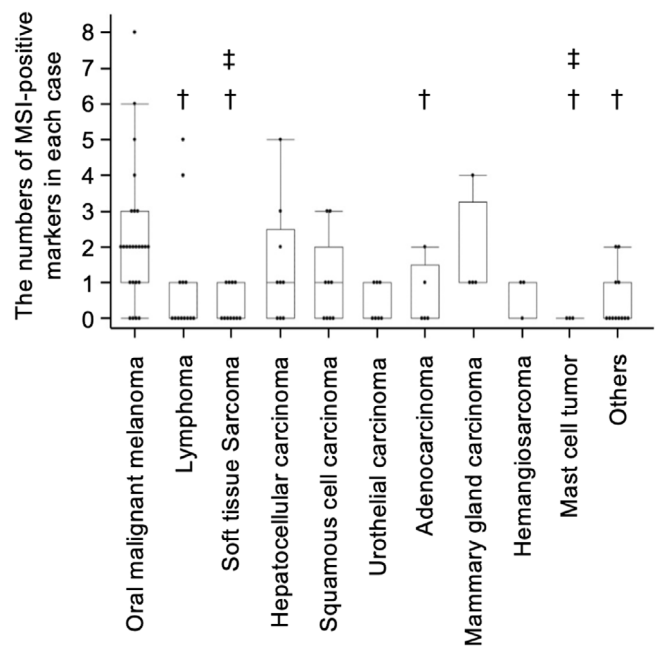
FIGURE 2 Number of MSI-positive markers across the multiple type sof canine tumors. All box-and-whisker plots represent the median (solid bars), interquartile range (boxes), and 1.5× interquartile range (vertical lines). † and ‡ show significant differences versus oral malignant melanoma and mammary gland carcinoma, respectively (Wilcoxon rank-sum test)
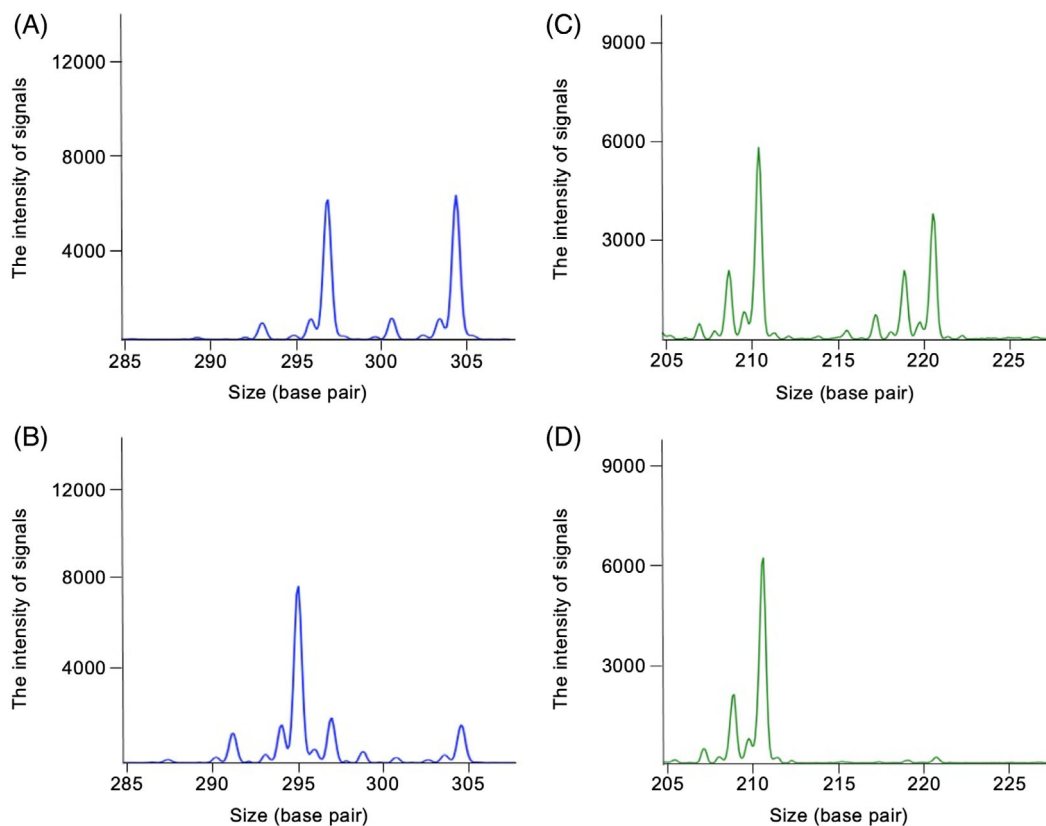
FIGURE 1 Representative electropherogram of fluorescently tagged PCR amplicons of FH2594 (A, B) and FH3113 (C, D) from normal (A, C) and tumor (B, D) DNA. The intensity of fluorescent signal is shown on the y-axis and the size of the PCR amplicons (base pairs) is shown on the x-axis. The alterations of peak size in (B) compared to (A) indicate microsatellite (MS) instability. The reduction of one allele in (D) compared to (C) indicates the loss of heterozygosity (LOH)

5 cases of lymphoma, 4 cases of soft tissue sarcoma, 6 cases of hepatocellular carcinoma, 5 cases of squamous cell carcinoma, 3 cases of adenocarcinoma, 2 cases of urothelial carcinoma, 4 cases of mammary gland carcinoma, 2 cases of hemangiosarcoma, and 4 cases of others, whereas no MSI-positive marker was detected in mast cell tumors (Figure 2). Oral malignant melanomas tended to have MSI markers more frequently.

Loss of heterozygosity was defined as a reduction in the peak of 1 allele in tumor DNA compared to that in normal DNA (Figure 1) and was evaluated for all MS loci. In addition, some cases showed increased amplitude of the other allele, which could indicate copy neutral LOH (CN-LOH). Copy loss LOH (no difference in amplitude of the other allele) was observed frequently in markers located in chromosome of *Canis lupus familiaris* (CFA) 5 (FH3837, FH2594, and FH3113), CFA 16 (FH2175), and CFA 22 (C22.763) across tumor types (Figure 3 and Table S1). Multiple MS markers on CFA 5 showed copy loss LOH in 4 cases (cases 22, 78, 89, and 93 in Table S1).

3.3 | Relationship between dMMR and MSI in clinical cases

The FFPE specimens of tumor tissues were obtained from 81 of 101 dogs. The canine MLH1, MSH2, and MSH6 (referred to cMLH1, cMSH2, and cMSH6) in these specimens were analyzed by IHC. The classifications of the 81 tumor specimens are shown in Table 3.

Representative results of IHC are shown in Figure 4A,B. Based on criteria for dMMR used in humans, all analyzed cases were classified into pMMR or dMMR. The proportion of tumors with dMMR was 8/21 (38.1%) cases of oral malignant melanoma, 1/4 (25%) cases of mammary gland carcinoma, 1/5 (20%) cases of urothelial carcinoma, and 3/9 (33.3%) cases of hepatocellular carcinoma, whereas the remainder of the specimens were classified into pMMR (Table 3 and Table S1). For 20 cases, including 2 dMMR cases (cases 1 and 46), out
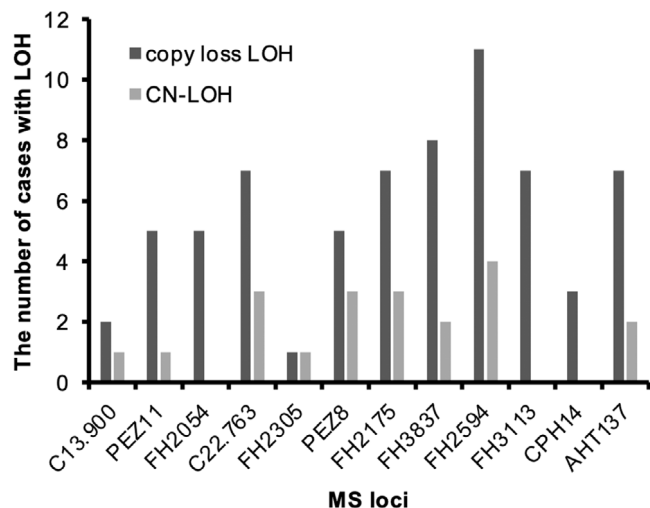
of 101 cases, FFPE samples of normal tissues also were available, and expression of MMR proteins was detected in all of them (Figure S1).

Then, whether or not dMMR was associated with MSI in clinical cases was confirmed. Comparing the number of MSI-positive markers between cases with dMMR or pMMR in entire tumors, these markers were significantly higher in cases with dMMR (Figure 4C, P < .0001). Further analysis of the relationship by tumor type identified significant results in oral malignant melanoma and hepatocellular carcinoma (P < .01 and P < .02, respectively) and entire tumors, but not in urothelial carcinoma and mammary gland carcinoma (P = .11 and P = .08, respectively). On the other hand, there was no relationship between dMMR and number of LOH (data not shown).

3.4 | Statistical evaluation to select MS loci suitable for dMMR/pMMR status

To identify which MSIs contributed substantially to dMMR in tumors of dogs, the LASSO regression model and decision tree analysis were used. In LASSO, 6 variables were estimated as nonzero coefficients (but not statistically significant), which might indicate that the appearance of MSI in FH2305 and the total number of MSI-positive markers reflect dMMR (Table 4).

Additionally, the decision tree model indicated that the cases with dMMR or pMMR could be classified with high probability by setting up nodes with ≥2 or ≤1 MSI-positive loci, respectively (Figure 5).

3.5 | Establishment of cell lines with dMMR and MSI analysis

We investigated whether dMMR induces MSI in vitro by canine cell lines after knockout of the MMR gene. A CRISPR/Cas9 system was used to establish the dMMR cell lines, and was followed by confirmation of knockout by Western blotting (Figure 6) and immunocytochemistry (Figure S2). No MLH1 protein was detected in both clones

FIGURE 3 Frequency of LOH in canine tumors by MS loci. The number of cases with LOH is shown on the y-axis, while the MS loci are shown on the x-axis. CN, copy neutral

TABLE 3 Mismatch repair status of tumor tissues in this study

Tumor type	Total cases	dMMR cases (%)
Oral malignant melanoma	21	8 (38)
Lymphoma	1	0
Mast cell tumor	2	0
Mammary gland carcinoma	4	1 (25)
Urothelial carcinoma	5	1 (20)
Hepatocellular carcinoma	9	3 (33)
Squamous cell carcinoma	9	0
Adenocarcinoma	7	0
Hemangiosarcoma	2	0
Soft tissue sarcoma	11	0
Others	10	0

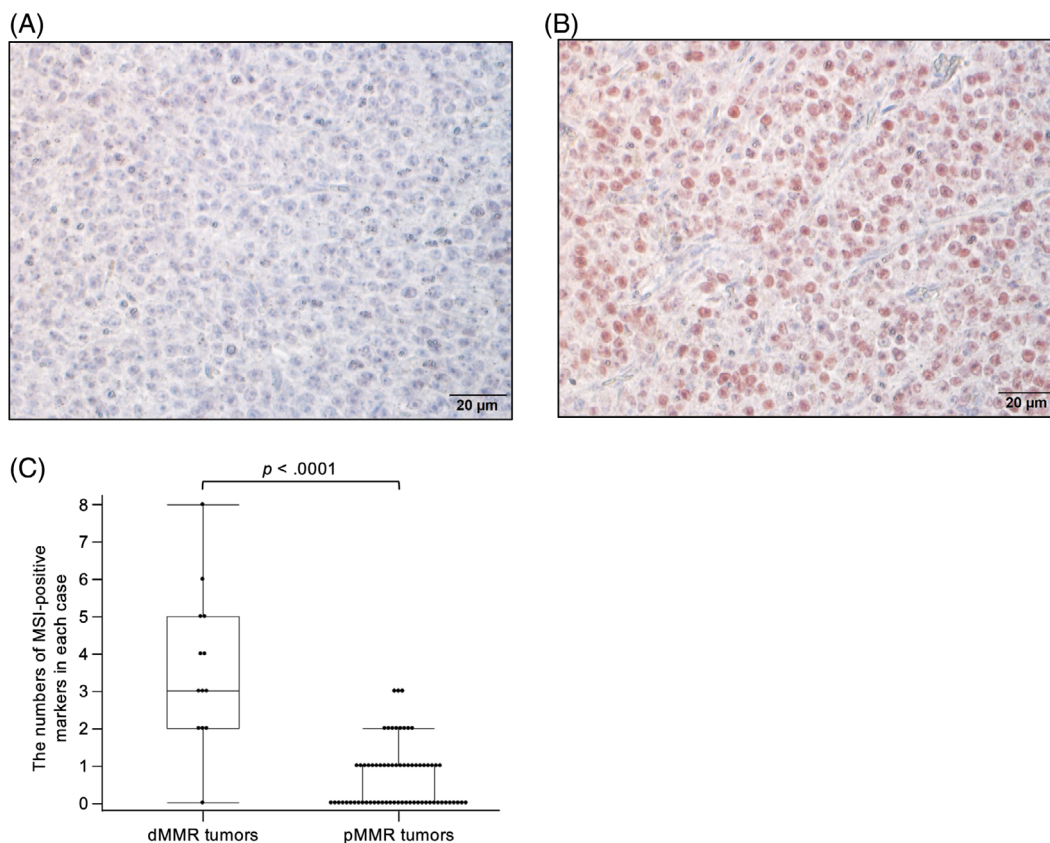Abbreviation: dMMR, mismatch repair deficiency.

FIGURE 4 Examples of immunohistochemistry demonstrating the loss of immunolabeling for cMLH1 (A) but retained immunolabeling for cMSH2 (B) in the nuclei of cells in a dog with oral malignant melanoma. These were counterstained with Mayer's hematoxylin. (C) Number of MSI-positive markers in each case by dMMR versus pMMR tumors ($P < .0001$, Wilcoxon rank-sum test). All box-and-whisker plots represent the median (solid bars), interquartile range (boxes), and $1.5\times$ interquartile range (vertical lines). dMMR, mismatch repair deficiency; pMMR, mismatch repair proficiency

Variants	Coefficients	Odds ratio	P-value	95% confidence interval
AHT137	1.21	3.34	.52	0.08-137.0
FH2305	1.27	3.57	.14	0.67-19.1
CPH14	0.87	2.38	.44	0.26-21.7
C13.900	1.26	3.52	.53	0.07-173.2
FH2175	−0.16	0.85	.86	0.14-5.35
Total MSI	0.33	14.2	.4	0.64-3.01

TABLE 4 Summary of LASSO regression model used to identify the variants associated with mismatch repair deficiency

of the MLH1 knockout cell line. The MSH2 and MSH6 knockout cell lines expressed no MSH6 and MSH2, in addition to defective expression of MSH2 and MSH6, respectively, as shown in a previous study.[4] The knocked-out cell lines and wild-type cells were serially passaged for 3 months to allow mutations to accumulate in MS loci. Then, the MSI status in these cell lines was analyzed at 2 time points (0 and 3 months). Based on results of the MSI analysis, an MSI-positive marker occurred in dMMR cell lines but not in wild-type cell lines from 0 to 3 months. At 3 months, 2 loci (FH2054 and AHT137) showed MSI in a cMLH1-deficient cell line, 2 loci (PEZ11 and FH3837) in a cMSH2-deficient cell line, and 4 loci (PEZ11, FH2054, FH2594 and AHT137) in a cMSH6-deficient cell line (Table 5).

4 | DISCUSSION

In this study, MSI and dMMR frequently were detected, mainly in canine oral malignant melanoma. A previous report by a different cohort indicated that oral malignant melanoma and hepatocellular carcinoma in dogs tended to have a defective MMR system,[4] which is consistent with our current study. In addition, we found that dMMR was related to MSI in both clinical cases and cell lines, which was supported by our results in the LASSO regression and decision tree model. However, the number of MSI-positive markers in the cell lines and some clinical cases with dMMR was lower than expected based on a previous study of humans showing that knockout of MMR genes
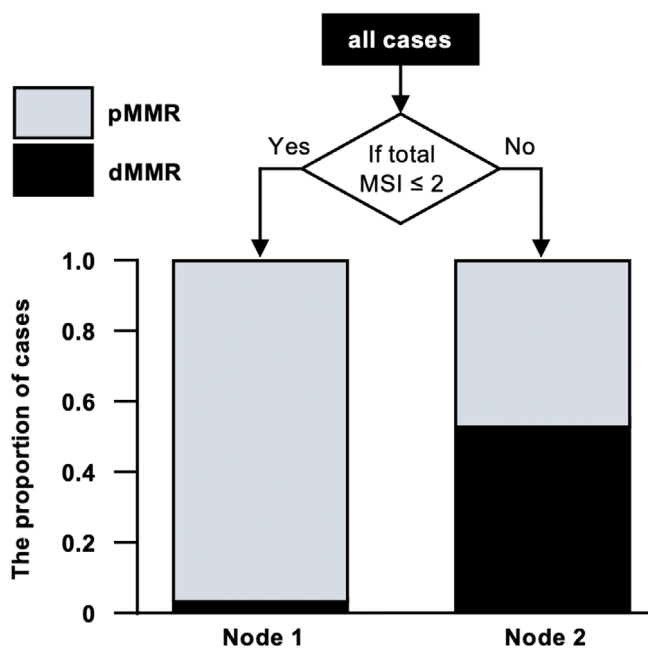
FIGURE 5 Results of the statistical models performed to select the variables associated with dMMR. The decision tree model was used to identify the variants most associated with the MMR status. At node 1, 59 patients with ≤2 MSI-positive markers were classified as a group with a high probability of pMMR. At node 2, 12 patients with ≥3 MSI-positive markers were classified as a group with a high probability of dMMR. The graphs attached to the decision tree demonstrate the ratio of the cases with pMMR or dMMR at each node
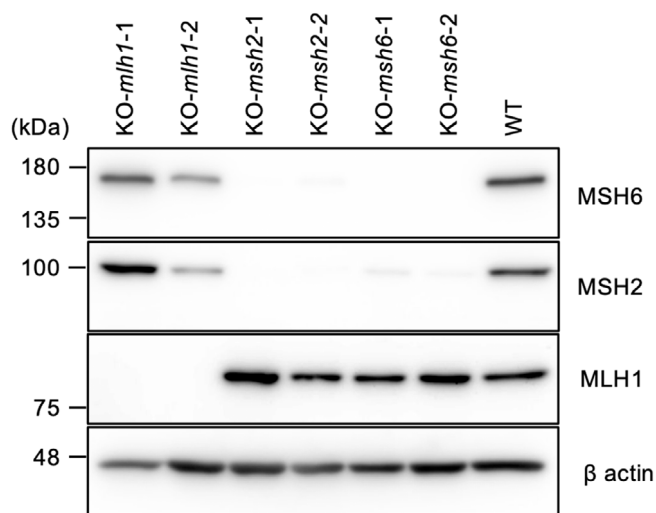

FIGURE 6 All cell lysates were prepared from SV40-immortalized canine gallbladder epithelial cells of the wild-type or with knockout of canine mismatch repair genes *mlh1*, *msh2*, and *msh6*. Two of each gene-knockout cell line were cloned and evaluated for the knockdown of proteins. Proteins were separated by SDS-PAGE, followed by western blotting by anti-human MLH1 antibody, anti-human MSH2 antibody, or anti-human MSH6 antibody. β-actin was used as a protein loading control

results in high frequencies of MSI.[28] There are several possible reasons for this difference: (a) presence of factors other than dMMR involved in the appearance of MSI; (b) other proteins that function as major MMR proteins; and (c) inappropriate MS loci used. Increased MS alterations at selected tetra-nucleotide repeats (IMAST) especially must be considered because 8 of all 12 MS loci used in our study were tetra-nucleotide repeat sequences (Table 1). The IMAST are caused by dysfunction of MSH3,[29] which is 1 of the MMR proteins, rather than that of MSH2, MSH6, MLH1, and PMS2. It was reported that IMAST occurring at tetra-nucleotide MS consisted of "AAAG" or "ATAG." In our study, 6 markers (PEZ11, FH2305, PEZ8, FH2175, FH3837, FH2594) consisted of "AAAG" repeats and 1 marker (FH2054) consisted of "ATAG" repeats. However, the expression of MSH3 proteins was not examined in our current study.

In humans, MSI is evaluated by analysis of 5 selected MS loci, and a tumor sample is defined as MS stable (MSS) if all 5 sequences are normal, MSI-low (MSI-L) if 1 sequence is mutated, or MSI-high (MSI-H) if ≥2 sequences are mutated. High microsatellite instability is highly consistent with dMMR in various tumors.[30,31] Several studies reported that tumors with dMMR/MSI-H have approximately 25 times more mutations than other tumors,[14] suggesting that tumors with dMMR/MSI-H express a number of neoantigens and are more immunogenic compared to tumors with pMMR/MSS or pMMR/MSI-L. Thus, it was expected that tumors with dMMR/MSI-H might be sensitive to ICIs, particularly for PD-1 or PD-L1 inhibitors. In fact, pembrolizumab, a PD-1 inhibitor used in humans was reported in clinical trials to be effective in patients with dMMR/MSI-H solid malignancies that progressed after chemotherapy, regardless of tumor type.[32-35] These results made pembrolizumab the first drug authorized for treatment based on MSI status rather than the pathological diagnosis.[36]

Recently, clinical trials of ICIs by canine PD-1 or PD-L1 inhibitors were reported in spontaneous tumors of dogs including oral malignant melanoma, and showed efficacy in some cases.[37-39] In these studies, some dogs with oral malignant melanoma experienced clinical benefits. Hence, in veterinary medicine, tumors with MSI/dMMR possibly could have a good response to PD-1 and PD-L1 inhibitors. Although few reports on ICI treatment for mammary gland carcinoma and hepatocellular carcinoma in dogs exist, studies evaluating its efficacy against these tumors are expected because of the high likelihood of MSI/dMMR.

As mentioned above, only 5 MS loci are used for MSI analysis in human medical practice. This MS panel is composed of mono- or di-nucleotide repeats because tri-nucleotide repeats are less altered than are mono- and di-nucleotide repeats.[40] Previous studies analyzed the MSI of multiple MS loci and MMR status and narrowed down the loci suitable for MSI analysis to 10 candidates.[40,41] Based mainly on these reports, the National Cancer Institute recommended an MS panel for MSI analysis and defined the border between MSI-H and MSI-L in 1998.[42] In our study, the appearance of MSI in C13.900, FH2054, CPH14, and AHT137 may particularly have relevance to dMMR however none of the results were significant. Lack of significance was probably a consequence of insufficient sample size. Moreover, our MS panel contained only a few di-nucleotide and no mononucleotide repeats. Furthermore, MSI analysis by mono- or di-nucleotide repeats

TABLE 5 Results of microsatellite analysis in canine mismatch repair genes-knocked out cell lines

Cell lines	Microsatellite markers											
	C13.900	PEZ11	FH2054	C22.763	FH2305	PEZ8	FH2175	FH3837	FH2594	FH3113	CPH14	AHT137
KO-*mlh1*			MSI									MSI
KO-*msh2*		MSI						MSI				
KO-*msh6*		MSI	MSI							MSI		MSI
Wild type							LOH					

Note: Blank cells indicates no alteration.

Abbreviations: LOH, loss of heterozygosity; MSI, microsatellite instability.

is needed if the influence of IMAST also is considered. The border between MSI-H and MSI-L in tumors of dogs also should be decided.

Furthermore, LOH frequently was identified in the markers located in CFA 5, 16, and 22, suggesting mutations of tumor suppressor genes in the same region. Copy loss LOH in MS loci suggests that inactivation of nearby tumor suppressor genes may contribute to carcinogenesis.[22] In fact, tumor suppressor genes *TP53*, *WRN*, and *RB1* are located in CFA 5, 16, and 22, respectively.[43] Thus, it was suspected that there were tumors with pMMR in our study caused by somatic deletion of the wild-type allele of these genes. Another study found that *TP53* is mutated in 16.7% of tumors in dogs,[44] which is similar to our results showing the detection of LOH at MS loci FH2594 in 15 cases. Tumor suppressor genes located in CFA 16 also may contribute to carcinogenesis. The CN-LOH was also detected sporadically across tumor types. Copy neutral loss of heterozygosity by mitotic recombination also can contribute to oncogenesis. For example, BRCA1/2 and Cyclin D1 are implicated in CN-LOH in tumors of humans.[45,46] In dogs, oncogenes also may be involved in the occurrence of CN-LOH. However, we did not evaluate expression of such tumor suppressor genes and oncogenes in our study, and more detailed studies are needed.

In our study, immunolabeling of PMS2 protein was not done because no monoclonal antibodies were certified to cross-react with canine PMS2 protein. In addition, the number of cases varied markedly depending on the tumor type. Because of the small number of cases of each tumor type, except for oral malignant melanoma, it will be necessary to recruit more tumor cases to evaluate the frequency of dMMR/MSI more accurately.

In conclusion, to our knowledge, ours is the first report in veterinary medicine to identify tumor types with frequent dMMR/MSI using a comprehensive analysis of dMMR and MSI. Our results also suggest a relationship between dMMR and MSI in clinical cases and in vitro. Additional studies are needed to consider other candidates.

CONFLICT OF INTEREST DECLARATION

Authors declare no conflict of interest.

OFF-LABEL ANTIMICROBIAL DECLARATION

Authors declare no off-label use of antimicrobials.

INSTITUTIONAL ANIMAL CARE AND USE COMMITTEE (IACUC) OR OTHER APPROVAL DECLARATION

Approved by the Ethics Committee of Yamaguchi University Animal Medical Center.

HUMAN ETHICS APPROVAL DECLARATION

Authors declare human ethics approval was not needed for this study.

ORCID

Takuya Mizuno https://orcid.org/0000-0002-9580-7557

REFERENCES

1. Tautz D. Notes on the definition and nomenclature of tandemly repetitive DNA sequences. *EXS*. 1993;67:21-28.
2. Poulogiannis G, Frayling IM, Arends MJ. DNA mismatch repair deficiency in sporadic colorectal cancer and Lynch syndrome. *Histopathology*. 2010;56(2):167-179.
3. McNiel EA, Griffin KL, Mellett AM, Madrill NJ, Mickelson JR. Microsatellite instability in canine mammary gland tumors. *J Vet Intern Med*. 2007;21(5):1034-1040.
4. Inanaga S, Igase M, Sakai Y, et al. Mismatch repair deficiency in canine neoplasms. *Vet Pathol*. 2021;58:1058-1063.
5. Li G-M. Mechanisms and functions of DNA mismatch repair. *Cell Res*. 2008;18(1):85-98.
6. Fishel R, Lescoe MK, Rao MR, et al. The human mutator gene homolog MSH2 and its association with hereditary nonpolyposis colon cancer. *Cell*. 1994;75:1027-1038.
7. Leach FS, Nicolaides NC, Papadopoulos N, et al. Mutations of a mutS homolog in hereditary nonpolyposis colorectal cancer. *Cell*. 1993;75(6):1215-1225.
8. Bronner CE, Baker SM, Morrison PT, et al. Mutation in the DNA mismatch repair gene homologue hMLH 1 is associated with hereditary nonpolyposis colon cancer. *Nature*. 1994;368(6468):258-261.
9. McGivern A, Wynter CVA, Whitehall VLJ, et al. Promoter hypermethylation frequency and BRAF mutations distinguish hereditary non-polyposis colon cancer from sporadic MSI-H colon cancer. *Fam Cancer*. 2004;3(2):101-107.
10. Mensenkamp AR, Vogelaar IP, van Zelst-Stams WAG, et al. Somatic mutations in MLH1 and MSH2 are a frequent cause of mismatch-repair deficiency in Lynch syndrome-like tumors. *Gastroenterology*. 2014;146(3):643-646.e8.

11. Umar A, Koi M, Risinger JI, et al. Correction of hypermutability, N-methyl-N'-nitro-N-nitrosoguanidine resistance, and defective DNA mismatch repair by introducing chromosome 2 into human tumor cells with mutations in MSH2 and MSH6. *Cancer Res*. 1997; 57(18):3949-3955.

12. Eshleman JR, Lang EZ, Bowerfind GK, et al. Increased mutation rate at the hprt locus accompanies microsatellite instability in colon cancer. *Oncogene*. 1995;10(1):33-37.

13. Eshleman JR, Markowitz SD. Mismatch repair defects in human carcinogenesis. *Hum Mol Genet*. 1996;5:1489-1494.

14. Le DT, Uram JN, Wang H, Bartlett BR, et al. PD-1 blockade in tumors with mismatch-repair deficiency. *N Engl J Med*. 2015;372(26):2509-2520.

15. Richman S. Deficient mismatch repair: read all about it (review). *Int J Oncol*. 2015;47(4):1189-1202.

16. Kumar R, Yu F, Zhen Y-H, et al. PD-1 blockade restores impaired function of ex vivo expanded CD8+ T cells and enhances apoptosis in mismatch repair deficient EpCAM+PD-L1+ cancer cells. *Onco Targets Ther*. 2017;13(10):3453-3465.

17. Diaz LA Jr, Le DT. PD-1 blockade in tumors with mismatch-repair deficiency. *N Engl J Med*. 2015;373(20):1979.

18. Coventry LL, Hosking JM, Chan DT, et al. Variables associated with successful vascular access cannulation in hemodialysis patients: a prospective cohort study. *BMC Nephrol*. 2019;20(1):197.

19. Yi M, Jiao D, Xu H, et al. Biomarkers for predicting efficacy of PD-1/PD-L1 inhibitors. *Mol Cancer*. 2018;17(1):129.

20. Engel E. A new genetic concept: uniparental disomy and its potential effect, isodisomy. *Am J Med Genet*. 1980;6(2):137-143.

21. O'Keefe C, McDevitt MA, Maciejewski JP. Copy neutral loss of heterozygosity: a novel chromosomal lesion in myeloid malignancies. *Blood*. 2010;115(14):2731-2739.

22. Eiriksdottir G, Sigurdsson A, Jonasson JG, et al. Loss of heterozygosity on chromosome 9 in human breast cancer: association with clinical variables and genetic changes at other chromosome regions. *Int J Cancer*. 1995;64(6):378-382.

23. Grundei T, Vogelsang H, Ott K, et al. Loss of heterozygosity and microsatellite instability as predictive markers for neoadjuvant treatment in gastric carcinoma. *Clin Cancer Res*. 2000;6(12):4782-4788.

24. Breen M, Jouquand S, Renier C, et al. Chromosome-specific single-locus FISH probes allow anchorage of an 1800-marker integrated radiation-hybrid/linkage map of the domestic dog genome to all chromosomes. *Genome Res*. 2001;11(10):1784-1795.

25. Guyon R, Lorentzen TD, Hitte C, et al. A 1-Mb resolution radiation hybrid map of the canine genome. *Proc Natl Acad Sci U S A*. 2003; 100(9):5296-5301.

26. Powierska-Czarny J, Miścicka-Sliwka D, Czarny J, et al. Analysis of microsatellite instability and loss of heterozygosity in breast cancer with the use of a well characterized multiplex system. *Acta Biochim pol*. 2003;50(4): 1195-1203.

27. Igase M, Shibutani S, Kurogouchi Y, et al. Combination therapy with reovirus and ATM inhibitor enhances cell death and virus replication in canine melanoma. *Mol Ther Oncolytics*. 2019;15:49-59.

28. Mandal R, Samstein RM, Lee K-W, et al. Genetic diversity of tumors with mismatch repair deficiency influences anti-PD-1 immunotherapy response. *Science*. 2019;364(6439):485-491.

29. Haugen AC, Goel A, Yamada K, et al. Genetic instability caused by loss of MutS homologue 3 in human colorectal cancer. *Cancer Res*. 2008;68(20):8465-8472.

30. Cicek MS, Lindor NM, Gallinger S, et al. Quality assessment and correlation of microsatellite instability and immunohistochemical markers among population- and clinic-based colorectal tumors results from the Colon Cancer Family Registry. *J Mol Diagn*. 2011; 13(3):271-281.

31. Yamashita H, Nakayama K, Ishikawa M, et al. Microsatellite instability is a biomarker for immune checkpoint inhibitors in endometrial cancer. *Oncotarget*. 2018;9(5):5652-5664.

32. Lemery S, Keegan P, Pazdur R. First FDA approval agnostic of cancer site—when a biomarker defines the indication. *N Engl J Med*. 2017; 377(15):1409-1412.

33. Le DT, Durham JN, Smith KN, et al. Mismatch repair deficiency predicts response of solid tumors to PD-1 blockade. *Science*. 2017;357(6349): 409-413.

34. Le DT, Kim TW, Van Cutsem E, et al. Phase II open-label study of pembrolizumab in treatment-refractory, microsatellite instability-high/mismatch repair-deficient metastatic colorectal cancer: KEYNOTE-164. *J Clin Oncol*. 2020;38(1):11-19.

35. Marabelle A, Le DT, Ascierto PA, et al. Efficacy of pembrolizumab in patients with noncolorectal high microsatellite instability/mismatch repair-deficient cancer: results from the phase II KEYNOTE-158 study. *J Clin Oncol*. 2020;38:1-10.

36. Marcus L, Lemery SJ, Keegan P, Pazdur R. FDA approval summary: pembrolizumab for the treatment of microsatellite instability-high solid tumors. *Clin Cancer Res*. 2019;25(13):3753-3758.

37. Igase M, Nemoto Y, Itamoto K, et al. A pilot clinical study of the therapeutic antibody against canine PD-1 for advanced spontaneous cancers in dogs. *Sci Rep*. 2020;10(1):18311.

38. Maekawa N, Konnai S, Nishimura M, et al. PD-L1 immunohistochemistry for canine cancers and clinical benefit of anti-PD-L1 antibody in dogs with pulmonary metastatic oral malignant melanoma. *NPJ Precis Oncol*. 2021;5(1):10.

39. Maekawa N, Konnai S, Takagi S, et al. A canine chimeric monoclonal antibody targeting PD-L1 and its clinical efficacy in canine oral malignant melanoma or undifferentiated sarcoma. *Sci Rep*. 2017;7(1):8951.

40. Dietmaier W, Wallinger S, Bocker T, Kullmann F, Fishel R, Rüschoff J. Diagnostic microsatellite instability: definition and correlation with mismatch repair protein expression. *Cancer Res*. 1997;57(21):4749-4756.

41. Bocker T, Diermann J, Friedl W, et al. Microsatellite instability analysis: a multicenter study for reliability and quality control. *Cancer Res*. 1997;57(21):4739-4743.

42. Richard Boland C, Thibodeau SN, Hamilton SR, et al. A National Cancer Institute workshop on microsatellite instability for cancer detection and familial predisposition: development of international criteria for the determination of microsatellite instability in colorectal cancer. *Cancer Res*. 1998;58(22):5248-5257.

43. Guevara-Fujita ML, Loechel R, Venta PJ, Yuzbasiyan-Gurkan V, Brewer GJ. Chromosomal assignment of seven genes on canine chromosomes by fluorescence in situ hybridization. *Mamm Genome*. 1996;7(4):268-270.

44. Alsaihati BA, Ho K-L, Watson J, et al. Canine tumor mutational burden is correlated with TP53 mutation across tumor types and breeds. *Nat Commun*. 2021;12(1):4670.

45. Beà S, Salaverria I, Armengol L, et al. Uniparental disomies, homozygous deletions, amplifications, and target genes in mantle cell lymphoma revealed by integrative high-resolution whole-genome profiling. *Blood*. 2009;113(13):3059-3069.

46. Walsh CS, Ogawa S, Scoles DR, et al. Genome-wide loss of heterozygosity and uniparental disomy in BRCA1/2-associated ovarian carcinomas. *Clin Cancer Res*. 2008;14(23):7645-7651.

SUPPORTING INFORMATION

Additional supporting information may be found in the online version of the article at the publisher's website.